Post-synthesis heat treatments of g-Fe2O3 nanoparticles embedded in a refractory matrix: From annealing of structural defects to doping

Charlotte Vichery, I Maurin, J.-P Boilot, T. Gacoin

Post-synthesis heat treatments of γ-Fe_2O_3 nanoparticles embedded in a refractory matrix: From annealing of structural defects to doping

C. Vichery,[a] I. Maurin, J.-P. Boilot, and T. Gacoin
Laboratoire de Physique de la Matière Condensée, CNRS-Ecole Polytechnique, UMR 7643, 91128 Palaiseau Cedex, France

(Presented 2 November 2011; received 22 September 2011; accepted 5 January 2012; published online 14 March 2012)

Magnetic nanoparticles (NPs) synthesized by low-temperature routes often present structural disorder, from extended defects to local rearrangements related to vacancy order or inversion in spinel ferrites. Post-synthesis heat treatments of preformed particles embedded in a refractory matrix are shown to modify magnetic anisotropy, either by annealing of crystal defects or by doping, while preserving the mean size and size distribution of the initial colloid. Such protected annealing of γ-Fe_2O_3 NPs allows a large and tunable increase of the anisotropy constant upon cobalt doping, using a two-step protocol that may involve adsorption of Co(II) ions at the surface of γ-Fe_2O_3 NPs followed by their dispersion in a silica matrix and heat treatments up to 600 °C. © *2012 American Institute of Physics*. [doi:10.1063/1.3680539]

I. INTRODUCTION

Nanoparticles of iron oxides exhibit unique magnetic properties which pave the way to various applications in nano- and biotechnologies, such as contrast agents for MRI or vectors for drug delivery and hyperthermia cancer treatment.[1] In order to reach optimum efficiency, each application requires specifically designed particles with tailored properties. Mean size, size distribution, saturation magnetization, and anisotropy constant are key parameters which have to be finely tuned. This paper reports on a versatile approach to modify one of these properties, namely the anisotropy constant, through the annealing of structural defects or cobalt doping while maintaining all other parameters fixed. It is well known that insertion of cobalt within the MFe_2O_4 spinel structure leads to an increased magnetic anisotropy;[2] the anisotropy constant of cobalt ferrite $CoFe_2O_4$ is about one order of magnitude larger than those of maghemite or magnetite. Co(II) ions can be readily adsorbed onto iron oxides, making them attractive for Co recovery from industrial wastes or natural water streams.[3,4] Salazar-Alvarez showed that post-synthesis adsorption of Co(II) onto maghemite nanoparticles led to a fourfold increase in coercivity.[5]

We have previously developed a strategy to improve the crystallinity of oxide-based NPs synthesized by low temperature routes, using post-synthesis heat treatments that preserve the narrow size distribution of the original colloid.[6] To achieve this, particles have first to be embedded in a refractory silica matrix to prevent aggregation and growth during annealing. In the present report, this approach is extended to γ-Fe_2O_3 and Co doped γ-Fe_2O_3 particles, using heat treatments up to 800 °C.

II. EXPERIMENT

(γ-Fe_2O_3:Co, mean size of 8 ± 2 nm, sample 1). Co doped γ-Fe_2O_3 NPs dispersed in SiO_2 were prepared using a multi-step procedure. At first, a colloid of magnetite NPs was synthesized by coprecipitation of Fe(II) and Fe(III) salts in alkaline medium.[7] 5.7 mL of ammonium hydroxide (13.3 M) were quickly added to 21 mL of an acidic solution of ferrous and ferric chlorides (0.48 M) under vigorous stirring. The precipitate of magnetite was then washed with distilled water before addition of 2.45 mL of nitric acid 2 M. After stirring, the excess of HNO_3 was discarded and 6 mL of a $Co(NO_3)_2$ aqueous solution (1.5 M) were added. The mixture was heated up to 130 °C for 30 min in order to oxidize magnetite into maghemite. The resulting particles were washed with distilled water, dispersed in HNO_3 solution at pH 2 and centrifuged four times to lower the size polydispersity. In a second step, the particles were embedded in a sol-gel SiO_2 matrix. An acidic solution of tetraethoxysilane (TEOS) in ethanol was first hydrolyzed and condensation was initiated by heating at 60°C for 1h. Different amounts of the γ-Fe_2O_3:Co ferrofluid were added to the sol, leading to composite materials with Fe/Si atomic ratio of 0.008 and 0.08. The mixtures were then dried in air at 100 °C until a xerogel was obtained. These composite powders were heated in air at different temperatures, ranging from 200 to 800 °C, for 1 h.

(γ-Fe_2O_3, mean size of 7 ± 2 nm, sample 2). For control measurements, maghemite NPs were synthesized following a protocol similar to the one previously described. The only difference was that $Fe(NO_3)_3$ (6 mL, 1.5 M) was used instead of $Co(NO_3)_2$ during the oxidation step.

Co doped reference NPs with a size of 7 ± 2 nm (sample 3) were also prepared in a similar way, except that Co ions were introduced during the precipitation stage. The quantity of $CoCl_2$ was adjusted to reach a Co content similar to that of sample 1. Note that KOH (13 M) was used instead of ammonium hydroxide to avoid the complexation of Co^{2+} ions. The as-obtained NPs were embedded in a silica matrix and heated in air at 600 °C for 1 h.

Powder x-ray diffraction patterns were recorded using a PANalytical XPert diffractometer equipped with Cu Kα radiation ($\lambda = 1.5418$ Å). Peak positions were refined individually and the lattice constant was determined by least-square refinement of the corresponding *d*-spacings. Note that an internal Si calibrant was used to obtain the lattice parameter value with high accuracy.

[a]Electronic mail: charlotte.vichery@polytechnique.edu.

The structural coherence length was evaluated through peak profile analysis using the Langford method,[8] after correction for the instrumental resolution function. The size distribution was also investigated by transmission electron microscopy (TEM) using a Philips CM30 microscope operating at 300 kV. Magnetization measurements were performed using a Cryogenic SX600 SQUID magnetometer. Samples were mounted in polycarbonate capsules with the ferrite powder dispersed in paraffin wax. Data were systematically corrected from the diamagnetic contributions of the silica matrix, wax and polycarbonate capsule. The iron and cobalt contents of the various composites were determined by elemental analysis using inductively coupled plasma-atomic emission spectroscopy. In sample 1, the Co/Fe atomic ratio was estimated to be 0.009 ± 0.002, whereas in sample 3, Co/Fe $= 0.011 \pm 0.002$.

III. RESULTS AND DISCUSSION

The size distribution of the γ-Fe_2O_3:Co NPs (sample 1) determined by TEM fits to a log-normal function with a mean diameter of 8.3 nm and a standard deviation of 2.0 nm. The x-ray diffraction pattern of the crude NPs is consistent with the *Fd3m* space group, which is adopted by magnetite, maghemite and cobalt ferrite. The coherence length value, L_c evaluated using the Langford method[8] is 7.1 ± 0.5 nm, i.e., close to the mean particle size derived from the TEM observations, indicating single-crystalline NPs. The value of the lattice parameter, $a = 8.352 \pm 0.003$ Å, is equal to that of bulk γ-Fe_2O_3 (JCPDS 39-1346). As this value departs from the one of bulk magnetite ($a = 8.396$ Å, JCPDS 19-0629), the NPs formed after the precipitation of Fe(II) and Fe(III) salts in alkaline medium can be considered as fully oxidized. The lattice constant, a was found to vary linearly with Co(II) insertion on the octahedral sites of the γ-Fe_2O_3 spinel structure.[9] It is likely that such a change could not be detected in the present case because of the very low Co content (Co/Fe = 0.009). Note that for samples 1 and 3, no secondary phases were evidenced by x-ray diffraction.

To prevent aggregation and growth during thermal treatments, NPs were dispersed in a microporous silica matrix prepared through sol-gel chemistry. Incorporation of the NPs in the matrix was achieved by addition of the ferrofluid into an acidic silica sol. Neither flocculation nor aggregation were observed after addition, leading to homogeneous composite powders after silica gelation and drying. X-ray diffraction (XRD) measurements were performed at first to monitor the structural and microstructural changes upon annealing from 100 to 800 °C. Composite samples with Fe/Si = 0.08 were used in order to get enough resolved diffraction patterns. The lattice parameter, a and coherence length values, L_c of the annealed samples are summarized in Table I. As previously reported for undoped γ-Fe_2O_3 NPs (sample 2),[10] no change in the lattice constant is observed upon heating confirming the complete $Fe_3O_4 \rightarrow \gamma$-$Fe_2O_3$ oxidation of the as-synthesized NPs. Besides, no full or even partial phase transformation into hematite occurs, at least up to 800 °C. Even though the $\gamma \rightarrow \alpha$-$Fe_2O_3$ transition temperature was found to increase with Co substitution,[9] the fact that the γ-Fe_2O_3 spinel structure is here maintained up to 800 °C is likely due to finite size effects and to the anti-sintering role of the matrix as previously reported.[10,11] Indeed, both L_c values

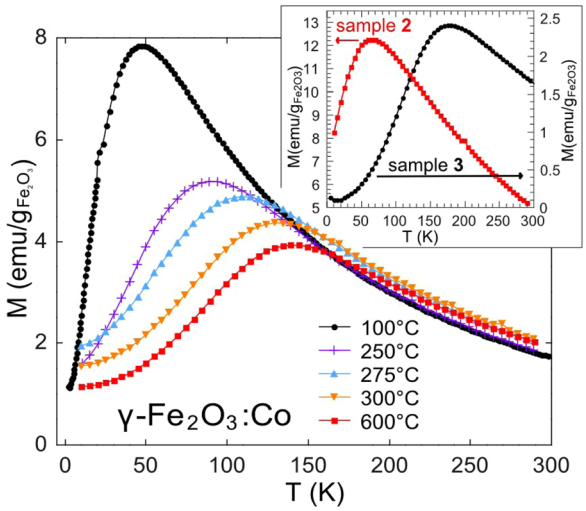

FIG. 1. (Color online) ZFC curves for γ-Fe_2O_3:Co NPs (1) embedded in silica (Fe/Si = 0.008) annealed at 100, 250, 275, 300, and 600 °C. In inset, ZFC curves for the γ-Fe_2O_3/SiO_2 composite (2) after drying at 100 °C and for sample 3. All measurements were performed under 25 G magnetic field.

(Table I) and TEM imaging support the absence of significant grain growth up to 600 °C for particles dispersed in silica.

Magnetization measurements were carried out on the γ-Fe_2O_3:Co NPs (1) embedded in silica using diluted (Fe/Si = 0.008) composites, so that magnetic dipole interactions and their possible change upon sintering of the SiO_2 matrix could be neglected. Zero Field Cooled (ZFC) measurements were recorded for samples annealed at 100, 250, 275, 300, and 600 °C (Fig. 1). The ZFC curves present a maximum, characteristic from the transition between the blocked and superparamagnetic states. The blocking temperature (T_B) at which this transition occurs is commonly related to the temperature of the maximum in the ZFC curve: T_B can be estimated to be 1.5 to 2.5 times smaller than T_{peak} depending on the size distribution of the NPs assembly.[12,13] The anisotropy constant K can be evaluated as $K = 25 k_B T_B / V$, assuming that $T_B = T_{peak}$. k_B is the Boltzmann constant and V the mean volume of the particles. According to the previous section, the size distribution should not change upon annealing up to 600 °C, so that the absolute value of K will not be exact but will allow a comparison between samples. As shown in Table II and Fig. 1, T_{peak} and K increase with the annealing temperature. This trend is confirmed by the $M(H)$ curves measured at 10 K, i.e., in the blocked regime, which shows a significant increase in the coercive field value, $\mu_0 H_c$ upon heat treatments (Fig. 2). Again, a direct comparison between $\mu_0 H_c$ values is relevant because the particle size remains unchanged.

TABLE I. Lattice parameter value, a and coherence length value, L_c for γ-Fe_2O_3:Co particles (1) embedded in silica (Fe/Si = 0.08) and annealed at selected temperatures.

Temperature (°C)	100	200	300	400	600
a (Å) (±0.003)	8.347	8.349	8.349	8.348	8.347
L_c (nm) (±0.5)	7.4	7.5	7.3	7.8	7.9

To assess the localization of Co atoms in sample 1, we compared the magnetic properties of the silica composite obtained after the drying stage with the corresponding γ-Fe_2O_3 (2) sample. Note that the mean particle sizes are similar for all samples (see the experimental section). For γ-Fe_2O_3 NPs embedded in silica (Fe/Si = 0.01), we previously reported a T_{peak} value of 65 K and a coercive field of 160 G at 10 K (see the inset of Figs. 1 and 2). The latter value is similar to that of the sample 1 dried at 100 °C (Table II), while it much strongly departs from that of the Co doped γ-Fe_2O_3 reference sample (3) prepared by direct coprecipitation of Co and Fe precursors followed by heat treatment. In that case, both $\mu_0 H_c$ (3260 G at 10 K) and T_{peak} (180 K) are strongly affected by the increased magnetic anisotropy that is likely associated to Co insertion in the spinel structure. These results suggest that in sample 1 after the drying stage, Co is either adsorbed at the particle surface or located within the first few atomic layers of the outer shell, which is considered as a virtually dead magnetic layer at least at room temperature.[14] Before heat treatments, the presence of Co slightly affects the overall magnetic properties of sample 1. The large changes reported for $\mu_0 H_c$ and T_{peak} values upon annealing are expected to originate from the diffusion of Co within the lattice, but other parameters might be involved such as an increased crystallinity. We shall thus briefly recall the results of preliminary studies performed on undoped γ-Fe_2O_3 NPs (2) upon thermal annealing.[10] Heating at or above 290 °C led to a partial vacancy ordering evidenced by synchrotron x-ray powder diffraction data complemented by FT-IR measurements. This enhanced crystallinity was accompanied by a slight decrease in saturation magnetization associated with an increased magnetic anisotropy. These counter-intuitive observations were consistent with a propagation of the shell of noncollinear spins toward the inner core. Comparison with Monte Carlo simulations[15] suggested that these effects were mainly driven by the increased surface anisotropy, probably related to surface reconstruction, and/or by enhanced antiferromagnetic interactions in the volume due to vacancy ordering. Anyhow, the resulting changes in the magnetic properties were very small as compared to those encountered in sample 1. For instance, γ-Fe_2O_3/SiO_2 composites displayed a coercivity of 200 G at 10 K and a T_{peak} value of 75 K after annealing at 540 °C. On the contrary, after annealing at 600 °C, the magnetic properties of sample 1 are close to those of the reference sample, treated at the same temperature but with a slightly higher Co/Fe ratio. Therefore, the large and gradual increase in magnetic anisotropy reported on heating for sample 1 is most likely due to Co diffusion and progressive insertion into the spinel structure. As a result, the Co dopants are stabilized against a possible release in weakly acidic solutions as reported after a mere adsorption of Co(II) ions.[4] Indeed, doped particles can be recovered in a colloidal state by dissolution of the amorphous silica matrix in HF, followed by washing with water and dispersion in HNO_3 at pH 2.

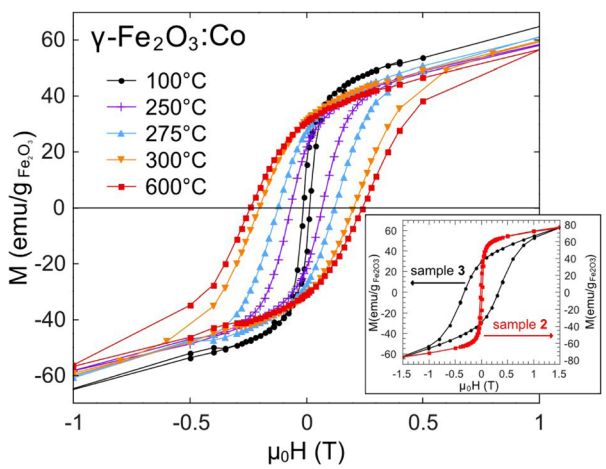

FIG. 2. (Color online) Magnetization vs magnetic field measured at 10 K for γ-Fe_2O_3:Co NPs (1) embedded in silica (Fe/Si = 0.008) after annealing at selected temperatures. In inset, $M(H)$ curves for the γ-Fe_2O_3/SiO_2 composite (2) after drying at 100 °C and for sample 3. Samples were cooled under zero magnetic field before measurements.

TABLE II. Parameters derived from the magnetic data for the γ-Fe_2O_3:Co (1)/SiO_2 composite (Fe/Si = 0.008) annealed at selected temperatures.

Temperature (°C)	100	250	275	300	600
$\mu_0 H_c$ (10 K) (G)	140	670	1210	2020	2400
T_{peak} (K)	47	90	110	131	142
K (10^6 erg cm^{-3})	0.54	1.04	1.27	1.51	1.64

IV. CONCLUSION

Post-synthesis heat treatments performed on γ-Fe_2O_3 NPs embedded in silica matrix afforded a control of their crystalline state, preventing both particle growth and transformation into hematite. The resulting increase in magnetic anisotropy was then limited to a slight change of the surface contribution presumably associated to a modification of the surface state. On the contrary, larger (up to 3 times) and tunable increase in the anisotropy constant could be achieved by cobalt doping, even at low levels (Co/Fe atomic ratio of 0.009), probably because of the large single-ion anisotropy of Co in octahedral environment. The doping protocol involved adsorption of Co(II) ions at the surface of γ-Fe_2O_3 NPs followed by dispersion in the SiO_2 matrix and annealing at temperatures ranging between 200 and 600 °C.

[1]G. C. Papaefthymiou, Nanotoday **4**, 438 (2009).
[2]J. C. Slonczewski, Phys. Rev. **110**, 1341 (1958).
[3]P. H. Tewari, A. B. Campbell, and W. Lee, Can. J. Chem. **50**, 1642 (1972).
[4]A. Uheida, G. Salazar-Alvarez, E. Björkman, Z. Yu, and M. Muhammed, J. Coll. Inter. Sci. **298**, 501 (2006).
[5]G. Salazar-Alvarez, J. Sort, A. Uheida, M. Muhammed, S. Suriñach, M. D. Baró, and J. Nogués, J. Mater. Chem. **17**, 322 (2007).
[6]G. Mialon, M. Gohin, T. Gacoin, and J.-P. Boilot, ASC Nano **2**, 2505 (2008).
[7]R. Massart, IEEE Trans. Magn. **MAG-17**, 1247 (1981).
[8]J. I. Langford, NIST Spec. Publ. **846**, 110 (1992).
[9]B. Gillot, F. Jemmali, and A. Rousset, J. Solid State Chem. **50**, 138 (1983).
[10]C. Vichery *et al.* (submitted to Chem. Mater.).
[11]C. Chanéac, E. Tronc, and J.-P. Jolivet, Nanostruct. Mater. **6**, 715 (1995).
[12]D. Peddis, C. Cannas, A. Musinu, and G. Piccaluga, J. Phys. Chem. C **112**, 5141 (2008).
[13]C. Cannas, A. Musinu, A. Ardu, F. Orrù, D. Peddis, M. Casu, R. Sanna, F. Angius, G. Diaz, and G. Piccaluga, Chem. Mater. **22**, 3353 (2010).
[14]H. Kachkachi, M. Noguès, E. Tronc, and D. A. Garanin, J. Magn. Magn. Mater. **221**, 158 (2000).
[15]O. Iglesias and A. Labarta, J. Magn. Magn. Mater. **290–291**, 738 (2005).